Degradation Patterns of GH11 xylanases for Efficiently Hydrolyzing xylan in Aspergillus Niger An76

Shu Zhang
Shandong University
Sha Zhao
Shandong University
Weihao Shang
Shandong University
Xiuyun Wu (wuxiuyun3353@163.com)
Shandong University https://orcid.org/0000-0002-5287-5218
Yingjie Li
Shandong University
Guanjun Chen
Shandong University
Xinli Liu
Qilu University of Technology
Lushan Wang
Shandong University

Research

Keywords: Aspergillus niger, GH11 xylanases, Transcription analysis, Degradation pattern, Synergistic hydrolysis

Posted Date: January 19th, 2021

DOI: https://doi.org/10.21203/rs.3.rs-148690/v1

Abstract

Background: Xylan is the most abundant hemicellulose polysaccharide in nature. Endo-xylanases from GH10 and GH11 families are the most critical xylan degrading enzymes. Filamentous fungi are highly effective xylan degraders and possess numerous xylan degrading isoenzyme-encoding genes, especially *Aspergillus niger*. Most noteworthy, the amplification of the GH11 xylanase-encoding genes occurs frequently in an organism, but the knowledge of each GH11 xylanases is little known.

Results: *A. niger* An76 encoded a comprehensive set of xylan-degrading enzymes, including five endo-xylanases (one GH10 and four GH11). Quantitative transcriptional analysis showed that three xylanases were up-regulated by xylose substrates, and the order and amount of enzyme secretion differed. Specifically, XynA and XynB were initially secreted successively, followed by XynC. Structural bioinformatics analysis indicated that the different modes of action of the three GH11 xylanases may be due to intricate hydrogen bonding between substrates and functional residues in the active site architectures. Heterologous expression and biochemical characterization of three GH11 xylanases (XynA, XynB and XynD) revealed differences in catalytic performance and product profiles. Furthermore, XynA and XynB displayed obvious synergistic action against beechwood xylan.

Conclusions: We investigated subtle differences in the functions of different isoenzymes in the same family using a combination of physiological and biochemical experiments. The transcriptional regulation and catalytic functions of enzymes could be the result of long-term evolutionary adaptation. The finding further expanded our understanding of GH-encoding genes amplification in filamentous fungi, which could guide the design of the optimal enzyme cocktails in industrial applications.

Background

Xylan is the most abundant hemicellulose polysaccharide in nature, accounting for about 20–35% of plant biomass [1]. It wraps around the outer layer of cellulose, together with lignin, resulting in “biomass recalcitrance” that makes plants resistant to microbial and enzymatic degradation [2–4]. Therefore, xylan must be degraded efficiently for the utilization of lignocellulose resources. The structure of xylan is composed of xylopyranosyl residues linked by β-D-1,4-glycosidic bond to form the main backbone, which is modified by various side-chain substituents such as L-arabinose, 4-O-methyl-glucuronic acid and acetyl group that are attached to the backbone in a variety of ways to form different bond types [1, 5]. The type and number of side-chain substituents vary in hardwoods (e.g., beechwood), herbaceous plants (e.g., wheat) and monocotyledons (e.g., corn) [6, 7]. According to the different structures of xylan substrates, microorganisms have evolved different xylan degradation systems, including a variety of xylan-degrading enzymes. Xylan could be converted to high-value products such as xylose, xylitol and xylooligosaccharides [8]. In particular, xylooligosaccharides are prebiotics that can stimulate the growth of human intestinal probiotics [9, 10], which have attracted much attention in the food and medical industries in recent years [11].

Endo-β-1,4-xylanases are the most critical enzymes in the degradation of xylan, breaking the β-1,4 glycosidic bond and producing different types of oligosaccharides [12], most of which belong to glycoside hydrolases (GH) 10 and 11 families. Studies on the genomes of filamentous fungi have revealed obvious xylanase genes amplification in both GH10 and GH11 families, which could encode xylanases of the same kind [13]. The structures and properties of GH10 and GH11 xylanases differ. GH10 xylanases adopt a $(\beta/\alpha)_8$-barrel fold, while the structures of GH11 xylanases are β-jelly roll [14, 15]. Studies have shown that GH10 xylanases have a higher affinity for the highly substituted xylan backbone, but the substrate specificity of GH10 xylanases is weaker than that of GH11 enzymes [16]. GH11 xylanases catalyse xylan degradation specifically, hence they are considered the dominant enzymes for the degradation of xylan. Moreover, they can easily access complex biomass due to their low molecular weight and high catalytic activity [17]. These enzymes cannot cleave glycosidic bonds at substituents, and due to their larger substrate-binding cleft, they preferentially degrade long-chain xylooligosaccharides [18, 19].

Aspergillus niger is one of the most important species in the degradation of hemicellulose [20], and GH11 xylanases are crucial. Gong et al. [21] reported that *A. niger* An76 possesses a complete lignocellulolytics enzyme system with diverse degrading enzymes according to genomic and proteomic analysis, particular for hemicellulases. In the process of degradation, the secretion of xylanases and side-chain degrading enzymes is in order and has a division of labor [21]. Two strategies have been proposed for the degradation of xylan from natural biomass by *Aspergillus fumigatus*: GH10 xylanase with carbohydrate-binding module 1 (CBM1) degrade the xylan near crystalline cellulose, and GH11 xylanases directly bind to and hydrolyse xylan in natural biomass [22]. Moreover, studies showed that GH10 xylanases containing CBM exert a strong synergistic effect with cellulases in the hydrolysis of pre-treated rice straw [23]. However, a lack of understanding of action mode and synergistic mechanism of GH11 xylanases secreted by the same organism, and the interaction mechanisms between enzymes of the same catalytic type and their substrate, has limited the exploitation of these enzymes.

In the present study, a physiological and biochemical combination approach was applied to explore multiple xylanases of *A. niger* An76 in xylan bioconversion. First, the transcription of various xylanase-encoding genes was analyzed by quantitative real-time PCR (qRT-PCR). Second, three GH11 xylanases were heterologously expressed and biochemically characterized to explore the different catalytic performances. Moreover, structural bioinformatic analysis was carried out to distinguish their degradation mechanisms. The results indicated that numerous xylanases secreted by an organism exhibited different modes of action toward different substrates and showed synergistic properties. The findings may contribute to the exploitation of glycoside hydrolases in industry.

Results

Quantitative transcriptional analysis of five xylanase-encoding genes cultured with different substrates

According to genome analysis, *A. niger* An76 possesses one GH10 xylanase (XynC) and four GH11 xylanases (XynA, XynB, XynD, and XynE; Additional file 1: Table S2). All the five xylanases contain signal peptides, hence they are secretory proteins. To elucidate the physiological relevant of these xylanases, quantitative transcriptional analysis was performed by qRT-PCR. Glycerol, xylose and xylooligosaccharide (XOS) were separately used as the sole carbon source to cultivate *A. niger* An76, and cells grew normally under all three carbon sources, with stable growth after 72 h (Additional file 1: Fig. S1). Samples cultured for 0, 6, 12, 24 and 48 h were selected to qRT-PCR analysis, and the results are shown in Fig. 1 and Additional file 1: Figure S2. Compared with glycerol as the carbon source, when cultured under xylose-like substrate, transcription of three xylanase genes (*xynA, xynB, and xynC*) was significantly increased, which indicated their importance to the degradation of xylan.

As shown in Fig. 1a, the relative transcription level of *xynA* was increased significantly at 6 h under xylose and XOS conditions. Expression of *xynB* was slightly behind that of *xynA*, and the overall transcription level was lower than that of *xynA* (Fig. 1b). In addition, the transcription level of *xynC* was increased at 24 h under xylose and XOS condition (Fig. 1c). Meanwhile, *xynD* and *xynE* were transcribed in small amounts or not at all (Fig. 1d and Additional file 1: Fig S2). Therefore, we speculated that XynA was initially expressed at high levels to degrade extracellular xylan, and its products further induced the expression of XynB. The GH10 xylanase XynC was secreted after the GH11 xylanase, and it could further degrade the degradation products of the former.

Bioinformatic analysis of differences in GH11 xylanase sequences and active site architecture

All characterised xylanases with PDB ID from eukaryota in the CAZy database (http://www.cazy.org/) were selected to construct a phylogenetic tree to improve the accuracy of subsequent structure prediction. Phylogenetic tree analysis indicated that xylanases comprise two main clades (GH10 and GH11, Fig. 2a). XynA, XynB and XynD clustered with GH11 family xylanases, and XynC clustered with GH10 family xylanases. In the GH11 family clade, XynB and XynD were located in one subclade, and XynA was located in another subclade. XynB and XynD were located on the same evolutionary branch, indicating that the evolutionary relationship between them is relatively close. Sequence alignment of three xylanases from GH11 family showed that XynB shared sequence identity of 65.48% with XynD, while XynA showed 52.07% and 45.03% amino acid sequence identity to XynB and XynD, respectively (Additional file 1: Fig. S3). Xylanases in the GH11 family had a conserved β-jelly roll structure, with a catalytic cleft that could accommodate six xylose moieties, and two key catalytic Glu residues (Fig. 2b). GH10 xylanases had a conserved $(\beta/\alpha)_8$-barrel structure and these enzymes also had two key catalytic Glu (Fig. 2c).

The catalytic functions of enzymes were closely related to their structures, especially active site architectures (Fig. 3). The intricate hydrogen bonding network formed between key functional amino acids and substrates in the active site architecture of members of the GH11 family was analyzed by structural bioinformatics. As shown in Fig. 3, the active sites of xylanases of the GH11 family could

accommodate six xylose units, but the interaction with the glycosylates could differ slightly. In the active site architecture of XynA, functional residues 17Tyr at the − 3 subsite and 75Ser, 184Ser at the + 3 subsite contributed to the binding of X6 (Fig. 3a). In contrast, interactions of XynB and XynD were mainly concentrated at the − 2 to + 2 subsites, which contained 4–5 additional interacting amino acids compared with XynA (Fig. 3b and 3c). These amino acids were 62Asn at the − 1 subsite, 90Tyr, 139Arg at the + 1 subsite, 196Tyr, 88Asn at the + 2 subsite in the active site architecture of XynB (Fig. 3b). Thus, we hypothesized that the degradation patterns of the three GH11 family isoenzymes differed somewhat, and this likely reflected different functions in the degradation of xylan.

Recombinant expression and enzymatic characterization of the three GH11 xylanases

To explore the biochemical properties and functions of the three GH11 xylanases, recombinant enzymes were cloned and expressed using *E. coli* expression system. The molecular masses of the three purified xylanases were determined by SDS-PAGE (Additional file 1: Fig. S4). The optimum temperature and optimum pH of the three recombinant xylanases were measured using 1% beechwood xylan as substrate. As shown in Fig. 4a and 4b, for all enzymes the optimum temperature was 50℃, and the optimum pH was 5.0. It is worth noting that XynB and XynD retained more than 60% of activity between 30 °C and 70 °C. Regarding thermostability, XynA and XynD exhibited 60% and 20% residual activity after 3 h incubation at 50℃, respectively. However, XynB was rapidly inactivated at 50℃ in 60 min (Fig. 4c). Regarding pH stability, the residual activity of the four xylanases was measured after incubation at pH 6.0. XynA and XynD retained more than 70% activity after incubated at pH 6.0 for 1 h, while XynB was relatively stable at pH 6.0, retaining ~ 80% activity after 1 h. After a 4 h incubation at pH 6.0, the residual activity of XynA, XynB and XynD gradually decreased to 40% (Fig. 4d).

Substrate specificities of the three xylanases were determined using two purified xylans (beechwood xylan and wheat arabinoxylan) and two natural biomass xylans (wheat bran and corn cob) as substrates. As shown in Additional file 1: Fig. S5, XynA, XynB and XynD displayed higher enzymatic activities toward purified xylans and lower enzymatic activity toward natural substrates. Among the three enzymes, XynB showed the highest enzyme activity. The activity of XynB with beechwood xylan was 6.7-fold higher than that of XynD and 8.2-fold higher than that of XynA. The activity of XynB with wheat arabinoxylan was ~ 5.8-fold higher than that of XynD and 10.8-fold higher than that of XynA. The specific activities of XynA, XynB, and XynD with beechwood xylan and wheat arabinoxylan are listed in Table 1.

Table 1
The kinetic parameters of the three recombinant xylanases.

Enzyme	Substrate	Specific activity (IU/mg)	V_{max} (μmol/min/mg)	K_m (mg/mL)	k_{cat} (s^{-1})	k_{cat}/K_m (mL/mg/s)
XynA	Beechwood xylan	139.9	1446.0	10.7	481.8	45.2
XynB	Beechwood xylan	1146.3	9330.0	3.0	3460.3	1140.9
XynD	Beechwood xylan	170.5	2813.0	5.4	1080.2	199.5
XynA	Wheat arabinoxylan	99.6	904.3	10.2	301.3	29.5
XynB	Wheat arabinoxylan	1019.3	5172.0	3.7	1918.2	512.3
XynD	Wheat arabinoxylan	160.8	1319.0	6.3	506.4	79.9

Kinetic parameters were determined for XynA, XynB and XynD using beechwood xylan and wheat arabinoxylan as substrates (Table 1). The catalytic kinetic parameters of the three xylanases were quite different. The K_m value of XynB was the smallest, followed by XynD, and the K_m value of XynA was the largest. This result indicated that the substrate binding ability of the three xylanases was ordered: XynB > XynD > XynA. XynB exhibited the largest k_{cat}, the smallest K_m, and the highest catalytic efficiency (k_{cat}/K_m), which is consistent with the determination of enzyme activity. The k_{cat}/K_m of XynB with beechwood xylan was 25.3-fold higher than that of XynA and 5.7-fold higher than that of XynD. The k_{cat}/K_m of XynB with wheat arabinoxylan was 17.3-fold higher than that of XynA and 6.4-fold higher than that of XynD. Moreover, XynA, XynB and XynD all displayed higher catalytic efficiency (k_{cat}/K_m) for beechwood xylan than wheat arabinoxylan, suggesting that the complexity of substrate structure is inversely proportional to enzyme activity.

Degradation pattern determination of the three GH11 xylanases

In order to explore the differences in degradation patterns of the three xylanases, X4、X6, beechwood xylan, wheat arabinoxylan, wheat bran, and corn cob were used as substrates for FACE analysis. Obvious differences in hydrolysis products were observed between xylan substrates (Additional file 1: Fig. S6). The main products of the degradation of beechwood xylan were xylooligosaccharides with a degree of polymerization (DP) below 5. The hydrolysis products of wheat arabinxylan contain more large oligosaccharides with DP greater than 5 and less X1, X2, X3. The hydrolysis products generated from wheat bran and corn cob were similar to those wheat arabinoxylan, except that the hydrolysate of XynB

contained fewer X4 and more X3. These results indicated that xylan containing more side chains inhibited degradation by all three GH11 xylanases, and more importantly, XynB might be advantageous for the degradation of XOS, especially X4.

In the degradation of X4 and X6, XynA degraded X6 faster than XynB and the main products were X2, X3 and X4 (Fig. 5a), which indicated that XynA had a preference for X6 degradation. The main products produced from X6 degradation by XynB were X2 and X3 (Fig. 5b). From these results, we speculated that XynB may rapidly degrade the produced X4 to generate X2. Analysis of the degradation of X4 confirmed our conjecture. XynA degraded some X4 within 5 min, and the content of X4 remained stable thereafter (Fig. 5c). In contrast, XynB and XynD continued to degrade X4 over 60 min, and the amount of X2 continued to increase (Fig. 5d). In addition, the degradation patterns of XynD on X4 and X6 were similar to those of XynB (Additional file 1: Fig. S7).

Synergistic hydrolysis of the three GH11 xylanases

In order to further elucidate the functions of the three GH11 isoenzymes XynA, XynB and XynD in the degradation of xylan, we conducted a synergistic hydrolysis experiment. As shown in Fig. 6, the degradation efficiency of the pairs of enzymes was higher than that of a single enzyme. Dual enzyme combinations displayed a significant synergistic effect and this was order XynA+ XynB >XynA + XynD > XynB + XynD (Fig. 6a). This result showed that the addition of either XynB and XynD could improve the degradation efficiency of XynA, which might be related to the degradation pattern of xylooligosaccharides. In addition, XynA + XynB (2 h) means that XynA is added to the beechwood xylan solutions for 2 h and then XynB with equal enzyme activity is added. This treatment resulted in the highest quantity of reducing sugars when (Fig. 6b), which indicated that the synergistic hydrolysis efficiency was greatly improved. This result is consistent with the physiological determination of the two xylanases, XynA was induced first by xylose-like substrate, followed by XynB.

Discussion

At the physiological level, all three xylanase genes in *A. niger* An76 were strongly induced under xylose-like subtrates (Fig. 1). In this process, XynA of the GH11 xylanase was the first enzyme to be upregulated, and the products induced the expression of XynB of the GH11 xylanase. XynC of the GH10 xylanase was secreted behind xylanases of the GH11 xylanase, and they can further degrade the products of the former enzymes. This may be related to the substrate specificities and degradation patterns of xylanases. Previous studies showed that GH10 xylanases can degrade the xylan near crystalline cellulose, which occurred after degradation of GH11 xylanases [22, 24]. Moreover, we also found that xylose could effectively induce xylanase genes transcription (Fig. 1). Xylose can effectively induce the transcription of xylanases by activating the transcription factor XlnR [25]. Analysis of XlnR binding sites in the 1000 bp transcription regulatory region revealed four XlnR binding sites in *xynA* and two XlnR binding sites in *xynB* (Additional file 1: Table S2) [26]. XynA and XynB may be directly dependent on regulation by XlnR

and continuously highly expressed. To elucidate the specific transcriptional regulation mechanism, genetic manipulation methods will be needed in future work.

Structural bioinformatics analysis revealed some differences in the sequences and active site architectures of the three GH11 xylanases. XynA appeared to be quite distantly related to XynB and XynD (Fig. 2a). Furthermore, the fine distribution of functional residues in active site architectures was diverse (Fig. 3), which might be related to individual degradation pattern. The hydrolysis products profiles of GH11 xylanases showed that XynA preferentially degraded X6 to produce X2, X3 and X4, while XynB and XynD preferentially degrade X4 (Fig. 5). This result correlated with the observed differences in the number of hydrogen bonds between functional amino acids in the active site architecture. The preference of XynA for X6 can be explained by hydrogen bonds at the − 3 and + 3 subsites, consistent with previous studies showing that increasing the binding energy of the enzyme at distal subsites can enhance the ability to degrade long oligosaccharides [27, 28]. In contrast, interactions of XynB and XynD were mainly concentrated in the − 2 to + 2 subsites, which resulted in strong binding of X4 [36]. Different hydrolysis products were generated by different family members [29], and members of the same family can also could produce different products due to the low sequence conservation of distal active subsites. Therefore, during long-term evolutionary adaptation, the fine distribution of functional amino acids in the active sites of isoenzymes in the same family leads to differences in the number of hydrogen bonds, which may lead to differences in the preference of enzymes for substrates and consequently the diversity of products.

Characterization of XynA, XynB and XynD revealed clear differences in enzyme activities (Additional file 1: Fig. S5 and Table 1). The activities of XynA, XynB and XynD with beechwood xylan were higher than those with wheat arabinoxylan, and far higher than those with natural biomass xylan. The degree of side chain substituents of beechwood xylan and wheat arabinoxylan was 12.8% and 38%, and the ratio of xylose to arabinose in natural substrates such as wheat bran was 0.7:1 [30]. Therefore, differences in enzyme activity with different substrates may be related to the structural complexity of substrates. These results are similar to those of a previous report on xylanase degradation of different xylan from *Streptomyces* sp. B6 [31]. Moreover, the enzyme activity of XynB was higher than that of XynA and XynD with all substrates. XynB engaged in strong binding interactions in -1, + 1 and + 2 subsites, and preferentially degraded small xyloligosaccharide such as X4 (Fig. 3 and Fig. 5). In addition,acid or alkali pretreatments can significantly improve biomass delignification and enhance enzymatic hydrolysis [32, 33]. Thus, XynB may be more suitable for degrading pretreated substrates, rather than applying all three xylanases of the GH11 family.

Although various studies on protein expression and biochemical characterization of isozymes members of the GH family have been reported [34, 35], but the different substrate preferences and response times of different isoenzymes have been largely ignored at the physiological level. The substrate preferences and response time is coevolved with different biochemical properties of enzymes, in particular with their degradation patterns. In the present work, we investigated the functional differences between isozymes of the GH11 family using physiological and biochemical approaches. First, the substrate preferences and

response times of isoenzymes were analyzed by quantitative transcription; Functional amino acids and interaction networks with substrates in the active site architecture of isoenzymes were then analyzed by structural bioinformatics; Finally, we performed biochemical characterization and synergistic hydrolysis of isoenzymes, including substrate degradation patterns.

Conclusions

This work explored subtle differences secretion regularity of xylanase isoenzymes *A. niger* An76, including comprehensive functional characterisation and three GH11 xylanases and their synergistic hydrolysis mechanisms. In *A. niger*, xylanase XynA with lower catalytic activity was secreted first, which preferentially bound and degraded oligosaccharides above X6; XynB with high enzymatic activity was then secreted to degrade X4 and other small oligosaccharides. These functional properties were compatible with the evolution of the active site architectures of the enzymes. The findings explained the efficient xylan degradation mechanism of *A. niger* An76, and may help to develop an efficient and environmentally friendly degradation strategy with reduced production costs.

This work explored not only the isoenzymes secretion regularity of GH11 xylanases in *A. niger* An76, but also the comprehensive functional characterization and of three GH11 xylanases and synergistic hydrolysis mechanism. XynA with lower catalytic activity was secreted first, which preferentially bound and degraded oligosaccharides above X6; XynB with high enzymatic activity was then secreted to degrade X4 and other small oligosaccharides. These functional properties were compatible with the evolution of the active site architectures of the enzymes. The findings explained the efficient xylan degradation mechanism of *A. niger* An76, and may help to develop an efficient and environmentally friendly degradation strategy with reduced production costs.

Methods

Strains and growth conditions

A. niger An76 (DDBJ accession no. BCMY00000000, DNA Data Bank of Japan) was used for enzyme gene amplifications. Cultivation of *A. niger* An76 was performed according to methods described previously [21, 36]. A 1% (w/v) solution of different carbon sources was added to the culture medium to induce the production of enzymes, including glycerol, xylose and XOS. Fresh conidia (1×10^6 /mL) were used to inoculate in 250 mL liquid medium in triplicate at 30°C and 200 rpm. For qRT-PCR experiments, washed mycelia, which were cultivated in the presence of 1% (w/v) glycerol as carbon source for 24 h as a reference sample (0 h), were transformed into the fresh media containing 1% (w/v) xylose or XOS as the sole carbon source for induction. Mycelia samples were collected at different sampling times (0, 6, 12, 24 and 48 h) and stored at -80°C. *Escherichia coli* strains BL21 (DE3) and DH5α (DingGuo, Beijing, China) were used for protein expression and gene cloning, respectively.

RNA isolation and cDNA synthesis

Mycelia sampled at each time point were used to extract total RNA and synthesize cDNA. Total RNA was extracted using TRIzol reagent (Sangon, Shanghai, China) and other regents including chloroform, isopropyl alcohol and ethanol (Dingguo) using the TRIzol method [37]. The cDNA was synthesized using 1 μg RNA as template and purified using the HiScript III RT SuperMix + gDNA wiper (Vazyme, Nanjing, China) according to the manufacturer's instructions.

qRT-PCR analysis of gene expression

qRT-PCR was performed using SYBR qPCR Master Mix (Vazyme) on LightCycler 480 instrument (Roche, Basel, Switzerland). The primers used to detect the expression levels of encoding genes are listed in Additional file 1: Table S1. Target genes included five xylanase genes (*xynA*, g9709.t1; *xynB*, g10033.t1; *xynC*, g1233.t1; *xynD*, g1345.t1; *xynE*, g3744.t1). The glyceraldehyde-3-phosphate dehydrogenase gene (*gapdh*, g7576.t1) was used as an internal reference gene. Error bars indicated the standard deviation. The concentration of cDNA template was 20 ng/μL. Relative transcription levels of target genes were calculated by the relative quantitation ($2^{-\Delta\Delta CT}$) method [38]. Three biological replicates and technical replicates were performed.

Gene cloning, enzyme expression and purification

Xylanase genes were cloned using PCR with synthesized cDNA as the template and primers listed in additional file 1: Table S1. PCR products were purified and cloned into a pLYJ-163 vector to construct recombinant plasmids, which were transformed into *E. coli* DH5α cells and confirmed by DNA sequencing (TSINGKE, Qingdao, China). The correct recombinant plasmids were transformed into *E. coli* BL21 (DE3) for protein expression. When the absorbance at 600nm (OD_{600}) reached 0.6-0.8, strains were induced using 0.5mM isopropyl-β-D-thiogalactopyranoside (IPTG, Solarbio, Beijing, China) for 20 h at 16℃. Cells were centrifuged and resuspended in buffer (50 mM NaH_2PO_4, 300 mM NaCl, pH 8.0). After ultrasonic fragmentation, xylanases were purified using HisCap Co 6FF resin (Smart-life Sciences, Changzhou, China). The eluent was replaced with optimal buffer (50 mM Na_2HPO_4, 20 mM citrate, pH 5.0) by ultrafiltration (3 kDa membrane, Millipore, Billerica, MA) at 4 °C. Pure enzymes were analysed by sodium dodecyl sulfate polyacrylamide gel electrophoresis (SDS-PAGE). Protein concentrations were determined using the Bradford method [39].

Enzymatic activity assay

Xylanase activity was assayed using the 3,5-dinitrosalicylic acid (DNSA) method [40]. A 40 μL volume of appropriately diluted XynA, XynB and XynD (5 μg/mL, 1 μg/mL and 5 μg/mL, respectively) were incubated with 60 μL 1% (w/v) xylan substrates. After incubation at 50 °C for 10 min, samples were mixed

with 80 µL of DNSA reagent, boiled immediately for 10 min, and subsequently cooled on ice. After adding 820 µL water, the absorbance were measured at 540 nm. One unit of xylanase activity (IU) was defined as the amount of enzyme (mg) that released 1 µmol of xylose per minute under the optimal assay conditions.

Effects of pH and temperature on xylanases

The optimal pH of xylanases was determined in the range of pH 3.0-10.0 (50 mM sodium citrate buffer, pH 3.0-8.0; 50Mm Glycine-NaOH buffer, pH 9.0-10.0) by adding beechwood xylan substrate and incubating for 10 min at 50℃ using the above activity assay method. The activity at the optimal pH was defined as 100%. The optimal temperature of xylanases was determined at temperatures ranging from 30 to 70℃ in sodium citrate buffer (pH 5.0). The activity at the optimal temperature was defined as 100%.

The temperature stability of xylanases was determined by measuring the remaining activity after incubating the enzymes at various times (0, 20, 40, 60, 120, 180 and 240 min) at 50°C in the absence of beechwood xylan in 50 mM sodium citrate buffer (pH 5.0). The activity without pre-incubation was defined as 100%. To assess pH stability, xylanases were incubated in pH 6.0 buffers at different times (0, 30, 60, 150, 240 min) before the addition of xylan to initiate the action. The remaining enzyme activities were determined under optimal conditions. These experiments were repeated three times.

Substrate specificity and determination of kinetic parameters

Substrate specificity of xylanases was investigated using different xylan substrates at 1% concentration, including beechwood xylan, wheat arabinoxylan (Megzyme, Wicklow, Ireland), xylan from wheat bran and corn cob extracted by alkaline pretreatment [41]. Solid material was washed, 0.7% NaOH was added at a ratio of 1:7, and samples were incubated at 60℃ for 2 h. The resulting mixtures were filtered and the filtrate was neutralized with HCl. Xylan was precipitated with absolute ethanol, dried, ground into a powder, and stored at room temperature for subsequent experiments. Reactions were performed in 50 mM sodium citrate buffer (pH 5.0) at 50℃ for 10 min.

The kinetic parameters (K_m and V_{max}) of the enzymes were determined by incubating with different concentrations of beechwood xylan and wheat arabinoxylan (0.2-2.4%) at 50℃ for 5 min. Parameters were calculated using nonlinear regression of the Michaelis-Menten equation with GraphPad Prism 8.0 [42]. All experiments were performed in triplicate.

Analysis of hydrolysis products.

Hydrolysis products of different xylan substrates were determined by fluorescence-assisted carbohydrate electrophoresis (FACE) experiments [43]. Hydrolysis products were obtained following the reaction of enzymes (20 IU/mL) with 1% substrates at a ratio of 1:1 (v/v) at 50℃. Samples were removed at different times (0, 5, 15, 30 and 60 min) and inactivated at 105℃ for 10 min to terminate the reaction. The supernatant were collected by centrifugation at 12,000 rpm for subsequent electrophoresis analysis. Xylose (X1), xylobiose (X2), xylotriose (X3), xylotetraose (X4), xylopentaose (X5), xylohexaose (X6) were used as standards.

Synergistic hydrolysis experiments

To investigate the synergistic effect among xylanases, for each xylanase, the amount of the enzyme with equal xylanase activity (0.3 IU/ml) towards beechwood xylan was used to experience. XynA, XynB and XynD were added singly or in pairs to 1% beechwood xylan. The release of reducing sugars were determined by the DNS method after incubation at 50℃ for 24 h. Samples were removed at intervals, and samples without enzyme served as controls.

Another method was used to determine synergy between XynA and XynB [22]. XynA was added into the substrate and incubated at 50℃ for 2 h, then XynA and XynB with equal xylanase activity were added to separate solutions to give XynA+ XynB and XynA+ XynA. The reducing sugars released under different conditions were detected upon incubation for 24 h. Samples without enzyme under the same conditions served as controls. All the above hydrolysis assays were performed in triplicate.

Bioinformatics analysis

Signal peptides were predicted using SignalP website (http://www.cbs.dtu.dk/services/SignalP/). Multiple sequence alignments were performed using CLUSTAL (http://www.clustal.org/). Phylogenetic analysis was performed using MEGA 5.0 with the Neighbor-Joining method and 1000 bootstrap replicates [44]. Homology modeling was carried out using SWISS-MODEL (https://swissmodel.expasy.org/). Suitable templates were identified, *Aspergillus niger* CBS 513.88 (PDB ID: 2QZ2), *Talaromyces funiculosus* IMI-134756 (PDB ID: 1TE1), *Talaromyces cellulolyticus* CF-2612 (PDB ID: 3WP3) were selected for XynA, XynB and XynD, respectively. Models were then generated based on each of the individual templates. The ligand in the enzyme-ligand complex of GH11 and GH10 was obtained from *Tr*Xyn11A (PDB: 4HK8) and *Geobacillus stearothermophilus* (PDB: 4PRW), respectively. Amino acid residues surrounding the substrate within 5 Å were selected to analyse the interactions between enzymes and substrates.

Abbreviations

GH: Glycoside hydrolase

CBM: Carbohydrate-binding module

XOS: Xylooligosaccharide

DP: Degree of polymerization

qRT-PCR: Quantitative real-time PCR

FACE: Fluorescence-assisted carbohydrate electrophoresis

X6: Xylohexaose

X5: Xylopentaose

X4: Xylotetraose

X3: Xylotriose

X2: Xylobiose

X1: Xylose

Declarations

Ethics approval and consent to participate

Not applicable.

Consent for publication

Not applicable.

Availability of data and materials

The data generated or analysed during this study are included in this published article and its additional information files. Further datasets used and analysed during the current study are available from the corresponding author on reasonable request.

Availability of data and materials

Not applicable

Competing interests

The authors declare that they have no competing interests.

Funding

The project was supported by the Key Research and Develop Program of Shandong Province (No. 2020CXGC010601) and Foundation of State Key Laboratory of Biobased Material and Green Papermaking□Qilu University of Technology□Shandong Academy of Sciences (No. GZKF202020).

Authors' contributions

SZ conducted the most of experiments and drafted the manuscript. SZ and WS participated in part of experiments and data analysis. YL, GC and LL revised the manuscript. XW and LW conceived the study and critically revised the manuscript.

Acknowledgements

We thank the Post-doctoral Funding of the State Key Laboratory of Microbiology Technology, Shandong University. We thank International Science Editing (https://www.internationalscienceediting.com) for editing this manuscript.

References

1. Smith PJ, Wang H-T, York WS, Peña MJ, Urbanowicz BR: Designer biomass for next-generation biorefineries: leveraging recent insights into xylan structure and biosynthesis. *Biotechnol Biofuels.* 2017;10(1):286-299.
2. Chundawat SPS, Beckham GT, Himmel ME, Dale BE: Deconstruction of lignocellulosic biomass to fuels and chemicals. *Annu Rev Chem Biomol Eng.* 2011;2(1):121-145.
3. Zhao X, Zhang L, Liu D: Biomass recalcitrance. Part I: the chemical compositions and physical structures affecting the enzymatic hydrolysis of lignocellulose. *Biofuel Bioprod Biorefin.* 2012; 6(4):465-482.
4. Rytioja J, Hildén K, Yuzon J, Hatakka A, de Vries RP, Mäkelä MR: Plant-polysaccharide-degrading enzymes from basidiomycetes. *Microbiol Mol Biol Rev.* 2014;78(4):614-649.
5. Moreira LRS, Filho EXF: Insights into the mechanism of enzymatic hydrolysis of xylan. *Appl Microbiol Biotechnol.* 2016;100(12):5205-5214.
6. Zhou X, Li W, Mabon R, Broadbelt LJ: A critical review on hemicellulose pyrolysis. *Energy Technol.* 2017;5(1):52-79.

7. Rogowski A, Briggs JA, Mortimer JC, Tryfona T, Terrapon N, Lowe EC, Baslé A, Morland C, Day AM, Zheng H *et al*: Glycan complexity dictates microbial resource allocation in the large intestine. *Nat Commun.* 2015;6(1):7481-7496.
8. Liu M, Huo W, Xu X, Weng X: Recombinant *Bacillus amyloliquefaciens* xylanase A expressed in *Pichia pastoris* and generation of xylooligosaccharides from xylans and wheat bran. *Int J Biol Macromol.* 2017;105:656-663.
9. Nordberg Karlsson E, Schmitz E, Linares-Pastén JA, Adlercreutz P: Endo-xylanases as tools for production of substituted xylooligosaccharides with prebiotic properties. *Appl Microbiol Biotechnol.* 2018;102(21):9081-9088.
10. Aachary AA, Prapulla SG: Xylooligosaccharides (XOS) as an emerging prebiotic: microbial synthesis, utilization, structural characterization, bioactive properties, and applications. *Int J Biol Macromol.* 2011;10(1):2-16.
11. Amorim C, Silvério SC, Prather KLJ, Rodrigues LR: From lignocellulosic residues to market: production and commercial potential of xylooligosaccharides. *Biotechnol Adv.* 2019;37(7):107397-107406.
12. Yu J, Liu X, Guan L, Jiang Z, Yan Q, Yang S: High–level expression and enzymatic properties of a novel thermostable xylanase with high arabinoxylan degradation ability from *Chaetomium* sp. suitable for beer mashing. *Int J Biol Macromol.* 2020;168:223-232.
13. Miia R M KSH, Ronals P. De V: Degradation and modification of plant biomass by fungi. *Fungal Genomics, 2nd Edition The Mycota XIII M Nowrousian (Ed) Springer-Verlag Berlin Heidelberg* 2014;8:175-208.
14. Javier AL-P, Anna A, Eva Nordberg K: Structural considerations on the use of endo-xylanases for the production of prebiotic xylooligosaccharides from biomass. *Curr Protein Pept Sci.* 2018;19(1):48-67.
15. Pell G, Taylor EJ, Gloster TM, Turkenburg JP, Fontes CMGA, Ferreira LMA, Nagy T, Clark SJ, Davies GJ, Gilbert HJ: The mechanisms by which family 10 glycoside hydrolases bind decorated substrates. *Curr Protein Pept Sci.* 2004;279(10):9597-9605.
16. Gong W, Zhang H, Tian L, Liu S, Wu X, Li F, Wang L: Determination of the modes of action and synergies of xylanases by analysis of xylooligosaccharide profiles over time using fluorescence-assisted carbohydrate electrophoresis. *Electrophoresis.* 2016;37(12):1640-1650.
17. Paës G, Berrin J-G, Beaugrand J: GH11 xylanases: structure/function/properties relationships and applications. *Biotechnol Adv.* 2012;30(3):564-592.
18. Biely P, Singh S, Puchart V: Towards enzymatic breakdown of complex plant xylan structures: State of the art. *Biotechnol Adv.* 2016;34(7):1260-1274.
19. Falck P, Aronsson A, Grey C, Stålbrand H, Nordberg Karlsson E, Adlercreutz P: Production of arabinoxylan-oligosaccharide mixtures of varying composition from rye bran by a combination of process conditions and type of xylanase. *Bioresour Technol.* 2014;174:118-125.
20. Li C, Zhou J, Du G, Chen J, Takahashi S, Liu S: Developing *Aspergillus niger* as a cell factory for food enzyme production. *Biotechnol Adv.* 2020;44:107630-107646.

21. Gong W, Dai L, Zhang H, Zhang L, Wang L: A highly efficient xylan-utilization system in *Aspergillus niger* An76: a functional-proteomics study. *Front Microbiol.* 2018;9:430-430.
22. Miao Y, Li P, Li G, Liu D, Druzhinina IS, Kubicek CP, Shen Q, Zhang R: Two degradation strategies for overcoming the recalcitrance of natural lignocellulosic xylan by polysaccharides-binding GH10 and GH11 xylanases of filamentous fungi. *Environ Microbiol.* 2017;19(3):1054-1064.
23. Inoue H, Kishishita S, Kumagai A, Kataoka M, Fujii T, Ishikawa K: Contribution of a family 1 carbohydrate-binding module in thermostable glycoside hydrolase 10 xylanase from *Talaromyces cellulolyticus* toward synergistic enzymatic hydrolysis of lignocellulose. *Biotechnol Biofuels.* 2015;8(1):77.
24. Shi Z, Han C, Zhang X, Tian L, Wang L: Novel synergistic mechanism for lignocellulose degradation by a thermophilic filamentous fungus and a thermophilic actinobacterium based on functional proteomics. *Front Microbiol.* 2020;11:539438.
25. Mach-Aigner AR, Pucher ME, Mach RL: Xylose as a repressor or inducer of xylanase expression in *Hypocrea jecorina* (*Trichoderma reesei*). *Appl Environ Microbiol.* 2010;76(6):1770-1776.
26. Gong W: Integrated functional-omics for assessment ofbiomass hydrolytic preference in important filamantous fungi [D]. China: Shandong University; 2017.
27. Zhang X, Wang S, Wu X, Liu S, Li D, Xu H, Gao P, Chen G, Wang L: Subsite-specific contributions of different aromatic residues in the active site architecture of glycoside hydrolase family 12. *Sci Rep.* 2015;5(1):18357-18368.
28. Wu X, Tian Z, Jiang X, Zhang Q, Wang L: Enhancement in catalytic activity of *Aspergillus niger* XynB by selective site-directed mutagenesis of active site amino acids. *Appl Microbiol Biotechnol.* 2018;102(1):249-260.
29. van Gool MP, van Muiswinkel GCJ, Hinz SWA, Schols HA, Sinitsyn AP, Gruppen H: Two novel GH11 endo-xylanases from *Myceliophthora thermophila* C1 act differently toward soluble and insoluble xylans. *Enzyme Microb Technol.* 2013;53(1):25-32.
30. Liu L, Gong W, Sun X, Chen G, Wang L: Extracellular enzyme composition and functional characteristics of *Aspergillus niger* An76 induced by food processing byproducts and based on integrated functional omics. *J Agric Food Chem.* 2018;66(5):1285-1295.
31. Liu L, Xu M, Cao Y, Wang H, Shao J, Xu M, Zhang Y, Wang Y, Zhang W, Meng X *et al*: Biochemical characterization of xylanases from *Streptomyces* sp. B6 and their application in the xylooligosaccharide production from viscose fiber production waste. *J Agric Food Chem.* 2020;68(10):3184-3194.
32. Wei W, Wang B, Wang X, Ling R, Jin Y: Comparison of acid and alkali catalyzed ethylene glycol organosolv pretreatment for sugar production from bagasse. *Bioresour Technol*. 2021;320:124293.
33. Zhao J, Tao X, Li J, Jia Y, Shao T: Enhancement of biomass conservation and enzymatic hydrolysis of rice straw by dilute acid-assisted ensiling pretreatment. *Bioresour Technol*. 2021;320:124341.
34. Du Y, Shi P, Huang H, Zhang X, Luo H, Wang Y, Yao B: Characterization of three novel thermophilic xylanases from *Humicola insolens* Y1 with application potentials in the brewing industry. *Bioresour*

Technol. 2013;130:161-167.

35. Lafond M, Guais O, Maestracci M, Bonnin E, Giardina T: Four GH11 xylanases from the xylanolytic fungus *Talaromyces versatilis* act differently on (arabino)xylans. *Appl Microbiol Biotechnol.* 2014;98(14):6339-6352.
36. Chen H, Gao P, Wang Z. Screening of high yield xylanase producing strain and studies on its submerged fermentation conditions. *Acta Microbiologica Sinica* 1990;(5):1-9.
37. Rio DC, Ares M, Hannon GJ, Nilsen TW: Purification of RNA using TRIzol (TRI reagent). *Cold Spring Harb Protoc.* 2010;2010(6):5439–5445.
38. Schmittgen TD, Livak KJ: Analyzing real-time PCR data by the comparative CT method. *Nat Protoc.* 2008;3(6):1101-1108.
39. Bradford MM: A rapid and sensitive method for the quantitation of microgram quantities of protein utilizing the principle of protein-dye binding. *Anal Biochem.* 1976;72(1):248-254.
40. Miller GL: Use of dinitrosalicylic acid reagent for detection of reducing sugars. *Anal Biochem.* 1959;31:426-428.
41. Rahmani N, Kahar P, Lisdiyanti P, Lee J, Yopi, Prasetya B, Ogino C, Kondo A: GH-10 and GH-11 Endo-1,4-β-xylanase enzymes from *Kitasatospora* sp. produce xylose and xylooligosaccharides from sugarcane bagasse with no xylose inhibition. *Bioresour Technol.* 2019;272:315-325.
42. Wu B, Zheng S, Pedroso MM, Guddat LW, Chang S, He B, Schenk G: Processivity and enzymatic mechanism of a multifunctional family 5 endoglucanase from *Bacillus subtilis* BS-5 with potential applications in the saccharification of cellulosic substrates. *Biotechnol Biofuels.* 2018;11(1):20-34.
43. Zhang Q, Zhang X, Wang P, Li D, Chen G, Gao P, Wang L: Determination of the action modes of cellulases from hydrolytic profiles over a time course using fluorescence-assisted carbohydrate electrophoresis. Electrophoresis. 2015;36(6):910-917.
44. Kumar S, Stecher G, Tamura K: MEGA7: molecular evolutionary genetics analysis version 7.0 for bigger datasets. *Mol Biol Evol.* 2016;33(7):1870-1874.

Figures

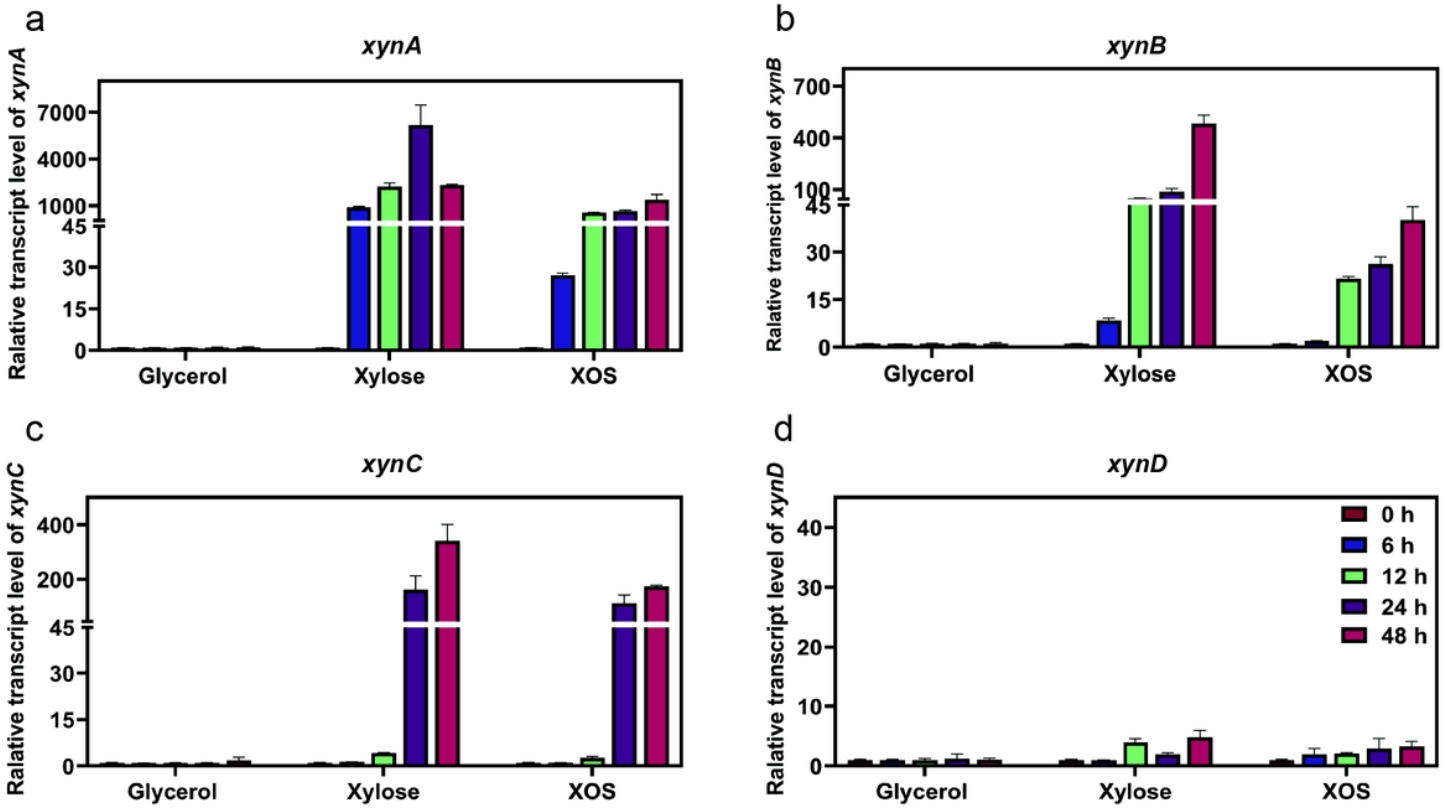

Figure 1

Relative transcript levels of four genes encoding xylanases in A. niger An76 induced by 1% glycerol, xylose and XOS. The transcript levels of xynA (a), xynB (b), xynC (c) and xynD (d) in A. niger An76 at different time points (0, 6, 12, 24 and 48 h). Glycerol served as a control. Relative transcript levels were calculated by the 2-ΔΔCT method. T-test analysis was used to calculate the significant differences in gene expression ($P < 0.05$).

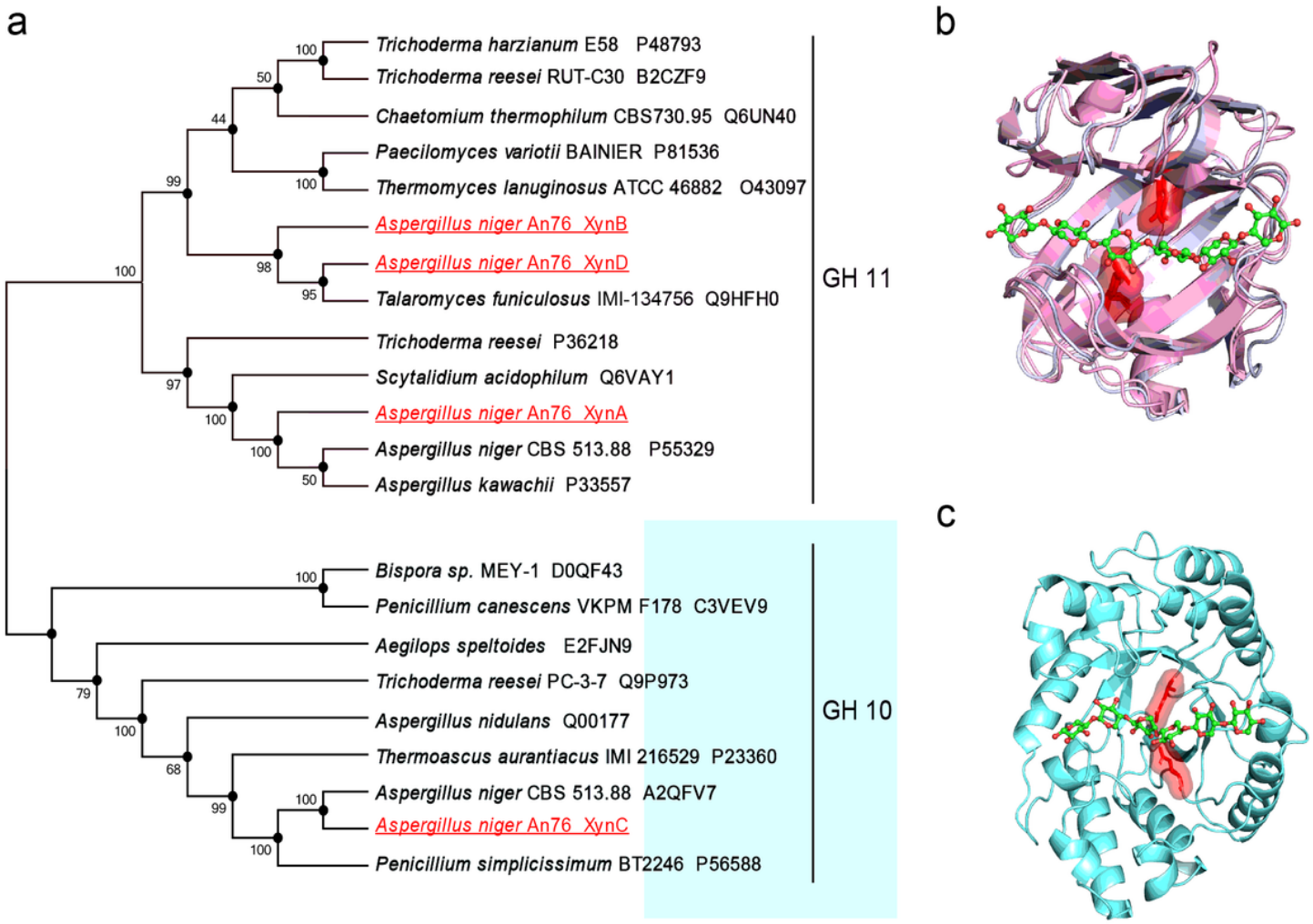

Figure 2

The phylogenetic tree and overall structures of GH11 and GH10 xylanases. a Phylogenetic tree resulting from the analysis of amino acid sequences of A. niger xylanases and other structurally characterized xylanases from Eukaryota constructed using the neighbor-joining method. Numbers on nodes correspond to the percentage bootstrap values for 1000 replicates. b The β-jelly roll structures of XynA, XynB and XynD from the GH11 family. c The (β/α)8-barrel structure of XynC from the GH10 family. The substrate sugar ring is represented by a sphere and green sticks. Catalytic amino acids are shown as red sticks.

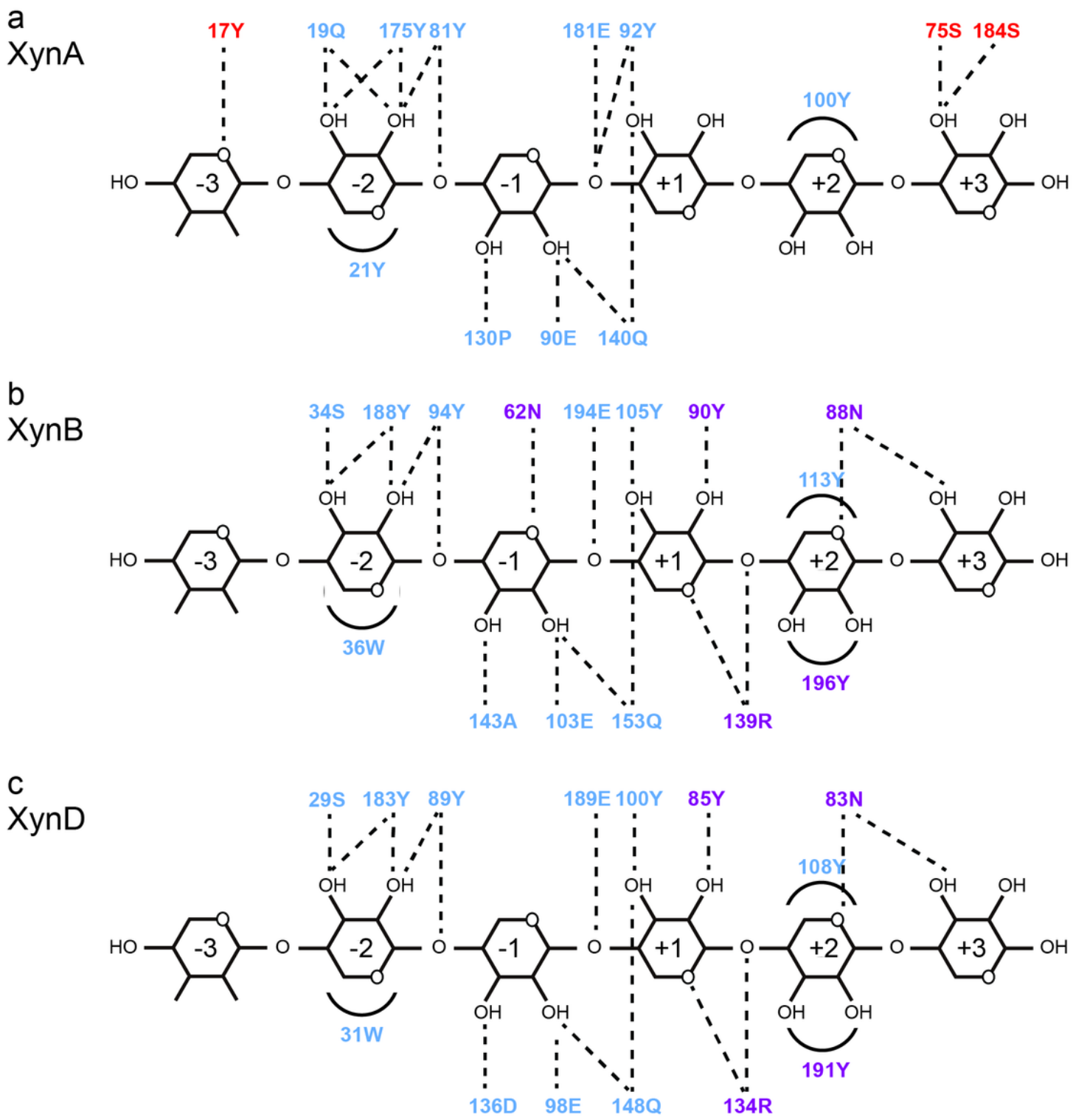

Figure 3

Schematic illustration of interactions between residues in the active site of XynA (a), XynB (b), XynD (c) and the xylohexaoses. Blue amino acids represent common interactions among the three xylanases. Red amino acids represent unique interaction residues of XynA. Purple amino acids represent he unique interaction residues of XynB and XynD. Dashed lines represent polar interactions, and arcs represent CH-π interactions.

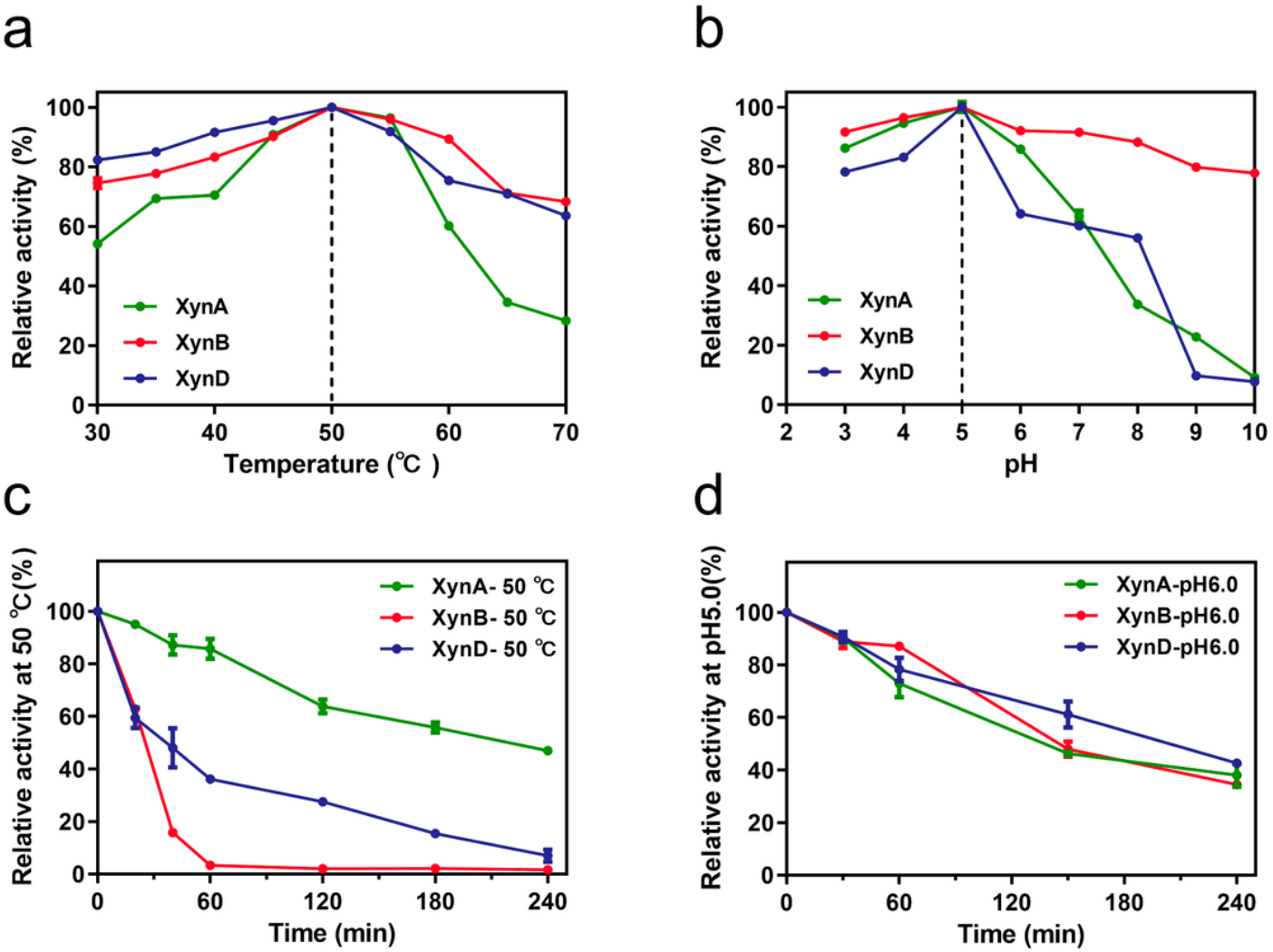

Figure 4

Effect of temperature and pH on the activity and stability of recombinant xylanases. a Effect of temperature on the activity of XynA, XynB and XynD. Enzymes were incubated at 30 to 70℃ for 10 min at pH 5.0. b Effect of pH on activity of XynA, XynB and XynD. Enzymes were incubated at pH 3.0 to 10.0 for 10 min at 50 ℃. c Temperature stability of XynA, XynB and XynD. Residual activities were measured under optimal conditions after incubation at 50 ℃ for different durations. d pH stability of XynA, XynB and XynD. Residual activities were determined under optimal conditions after incubation at pH 6.0 for different durations.

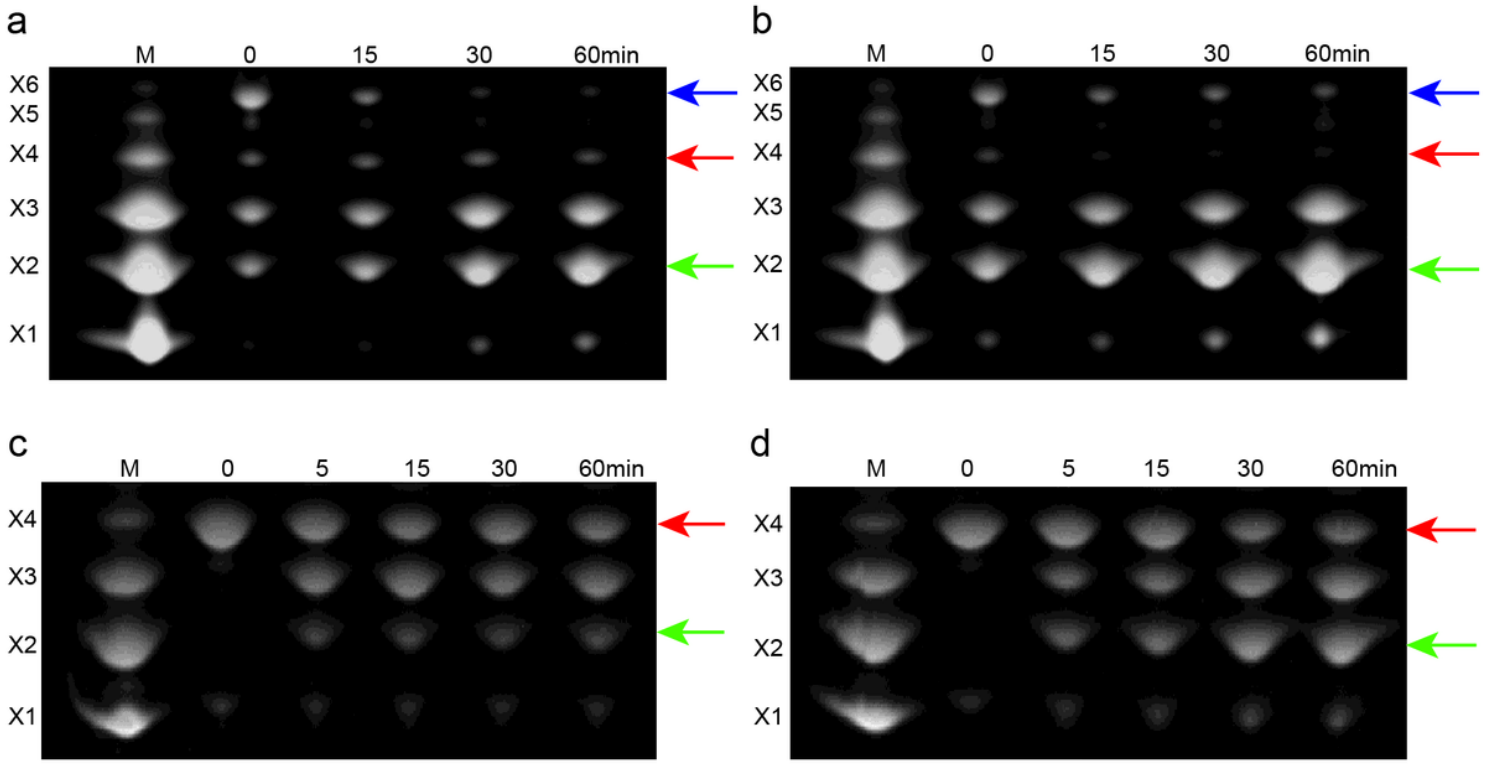

Figure 5

FACE analysis of products following hydrolysis of xylohexaose (a, b) and xylotetraose (c, d). a and b correspond to the products of xylohexaose hydrolyzed by XynA and XynB, respectively. c and d correspond to the products of xylotetraose hydrolyzed by XynA and XynB, respectively. Xylose (X1), xylobiose (X2), xylotriose (X3), xylotetraose (X4), xylopentaose (X5), xylohexaose (X6). Blue arrows indicate X6, red arrows indicate X4, and green arrows indicate X2.

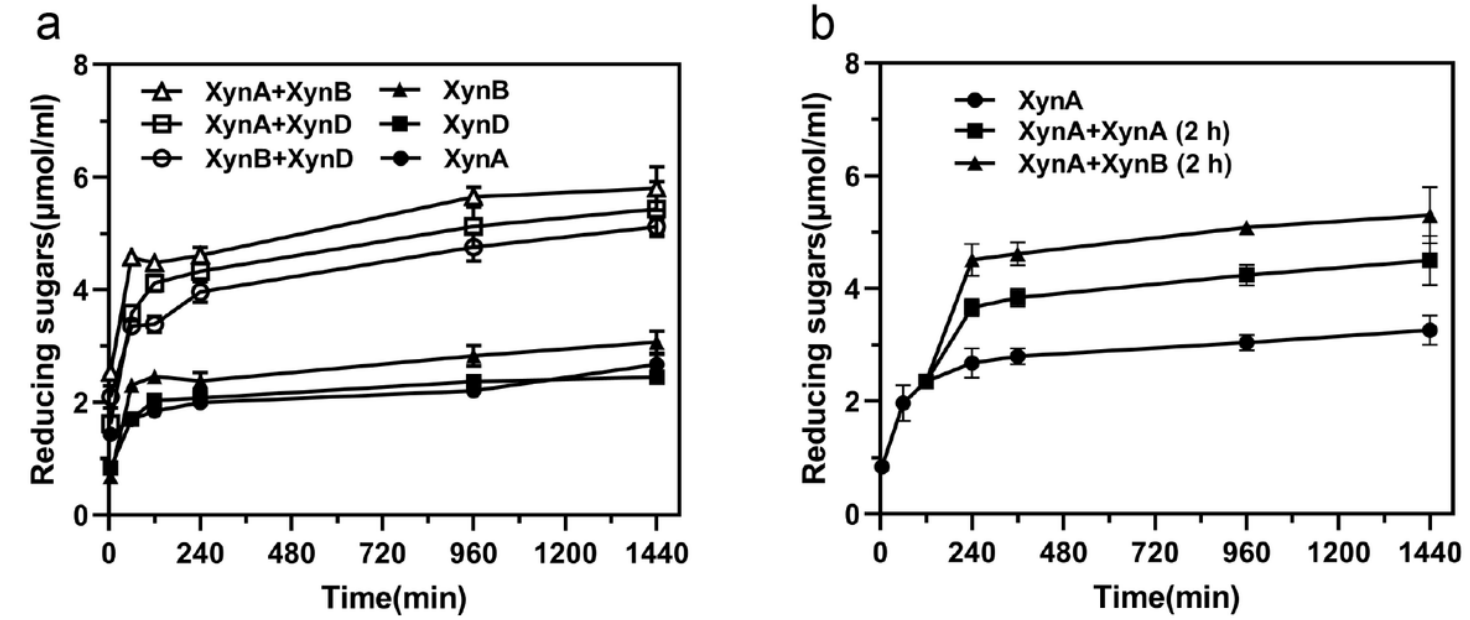

Figure 6

Hydrolysis synergy determination of the three GH11 xylanases. a Release of reducing sugars from beechwood xylan by the three xylanases, XynA, XynB, XynD alone or in combination. b XynA was added to the beechwood xylan substrate solutions in advance for 2 h, then XynA and XynB was added to give XynA + XynA (2 h) and XynA + XynB (2 h).

Supplementary Files

This is a list of supplementary files associated with this preprint. Click to download.

- Additionalfile1.docx